AIAA 80-1209R

Turbulent Flow Analysis of Erosive Burning of Cylindrical Composite Solid Propellants

M. K. Razdan* and K. K. Kuo†
The Pennsylvania State University, University Park, Pa.

An axisymmetric turbulent boundary layer was analyzed in order to investigate erosive burning in composite solid-propellant rocket motors. It was found that there is a strong interaction between the core flow acceleration and turbulence level in the boundary layer. The increase of turbulence near the surface of the propellant plays an important role in the erosive burning mechanism. Reducing the port diameter makes a rocket motor more sensitive to erosive burning. When the port diameter is uniform, the erosive burning rate increases toward the aft end of the rocket motor. This trend is less pronounced or even reversed when the port diameter is divergent.

Nomenclature

a = pre-exponent in strand-burning-rate law, (cm/s)/(MPa)^n
A = cross-sectional flow area
A_s = Arrhenius frequency factor in propellant surface decomposition, m/s
A^+ = damping constant in van Driest's hypothesis
$C_1 \rightarrow C_4, C_\mu, C_\omega$ = constants in turbulence models
C_P $\equiv \sum_k Y_k C_{Pk}$, average heat capacity of reacting gases, kcal/kg-K
C_{Pk} = heat capacity of kth species, kcal/kg-K
C_s = heat capacity of solid propellant, kcal/kg-K
d_{AP} = average diameter of ammonium perchlorate particles, m
D = port diameter of rocket motor, m
$\mathfrak{D}$ = diffusion coefficient in Fick's law, m^2/s
E_{as} = activation energy in propellant surface decomposition, kcal/mole
$\Delta h^\circ_{f,k}$ = heat of formation of kth species, kcal/kg
h_k $\equiv \Delta h^\circ_{f,k} + \int_{T^0}^{T} C_{Pk}\,dT$, static enthalpy of kth species, kcal/kg
H $\equiv \sum_k Y_k h_k + u_i u_i/2$, stagnation enthalpy of gases, kcal/kg
k = von Kármán's constant
K = $\overline{u_i' u_i'}/2$, turbulent kinetic energy, m^2/s^2
ℓ = mixing length, m
n = exponent in strand-burning-rate law
P = pressure, Pa
Pr $\equiv C_P \mu/\lambda$, Prandtl number based upon molecular properties of fluid
Pr_t = Prandtl number for turbulent flow
$\dot{Q}_r$ $\equiv (1/\nu_F W_F) \sum_k \nu_k W_k \Delta h^\circ_{f,k} \bar{\omega}_k$, rate of heat generation in gas phase, kcal/m^3·s
r = coordinate in radial direction, m
r_b = total burning rate of a solid propellant, m/s
r_{b_0} = strand burning rate of a solid propellant, m/s
R = port radius of rocket motor, m
R_h = roughness height, m
R_u = universal gas constant, N·m/kmole·K
Sc $\equiv \mu/\bar{\rho}\mathfrak{D}$, Schmidt number based upon molecular properties of fluid
Sc_t = Schmidt number for turbulent flow
T = temperature, K
T_{ci} = initial centerline temperature, K
T° = reference temperature, 298.14 K
T_p = propellant temperature, K
T_{pi} = propellant initial temperature, K
T_{ps} = propellant surface temperature, K
T_{ti} = initial stagnation temperature, K
$\bar{T}_{ps}$ = reference surface temperature of propellant, K
u = gas velocity in x direction, m/s
U = axial velocity outside boundary layer, m/s
U_{ci} = initial centerline velocity, m/s
u_* $\equiv \sqrt{\tau_w/\rho_\infty}$, friction velocity, m/s
v = gas velocity in y direction, m/s
W $\equiv \left(\sum_k Y_k/W_k\right)^{-1}$, average molecular weight of gases, kg/kmole
W_k = molecular weight of kth species, kg/kmole
x = coordinate in axial direction, m
y = coordinate normal to propellant surface, m
y_w $\equiv R$-y, coordinate with its origin on propellant surface, m
Y_k = mass fraction of kth species
Y_{FS} = mass fraction of fuel in a composite solid propellant
Y_{OS} = mass fraction of oxidizer in a composite solid propellant
$\bar{(\ )}$ = time-averaged quantity
$(\ )'$ = fluctuating quantity

Presented as Paper 80-1209 at the AIAA/SAE/ASME 16th Joint Propulsion Conference, Hartford, Conn., June 30-July 2, 1980; submitted Sept. 16, 1980; revision received June 12, 1981.

*Assistant Professor, Department of Mechanical Engineering. (Presently Research Engineer, Exxon Research and Engineering Company, Linden, N.J.) Member AIAA.

†Associate Professor, Department of Mechanical Engineering. Associate Fellow AIAA.

$( )_{,i}$ = partial differentiation of quantity in ( ) with respect to x_i, ( )/m
α = angle of divergence of port radius
δ = boundary-layer thickness, m
ϵ $\equiv \mu u'_{i,j} u'_{i,j}/\bar{\rho}$, turbulent dissipation, m^2/s^3
γ = constant-pressure to constant-volume specific heat ratio
λ = thermal conductivity of gas, kcal/m·s·K
λ_s = thermal conductivity of solid propellant, kcal/m·s·K
μ = gas viscosity, kg/m·s
μ_{eff} $\equiv \mu + \mu_t$, effective viscosity, kg/m·s
μ_t = turbulent viscosity defined in Eq. (8), kg/m·s
$(\mu/Pr)_{\text{eff}}$ $\equiv \mu/Pr + \mu_t/Pr_t$, kg/m·s
$(\mu/Sc)_{\text{eff}}$ $\equiv \mu/Sc + \mu_t/Sc_t$, kg/m·s
ν_k = number of kmoles of kth species
ρ = gas density, kg/m^3
ρ_s = solid propellant density, kg/m^3
τ $\equiv \mu_{\text{eff}} \partial\bar{u}/\partial y$, local shear stress, N/m^2
$\dot{\omega}_k$ = rate of production of species k due to chemical reactions, $kg/m^3 \cdot s$

Subscripts

b = bulk or averaged variable
c = centerline condition
k = species index representing fuel gas [F], oxidizer gas [O], and product gas [P]
∞ = freestream condition
w = wall (propellant surface) condition

Introduction

INTEREST in nozzleless and other high-performance rocket motors with low port-to-throat area ratios has stimulated the need for a better understanding of the erosive burning characteristics of solid propellants. Crossflow gas velocity within these rocket motors can reach sonic and even supersonic speeds over some portions of the propellant surfaces, leading to high augmentation of the burning rate of a solid propellant. This augmentation, caused by the crossflow of gases, is referred to as the erosive burning phenomenon.

Because previous studies on erosive burning have been reviewed by Kuo and Razdan[1] and King[2] and a summary and classification of various erosive burning theories has been presented by Razdan and Kuo,[3] no literature review is given in this paper. A theoretical model, in which a chemically reacting two-dimensional turbulent boundary layer was analyzed to predict erosive burning rates of composite solid propellants, was recently developed by the authors.[3] Predicted results showed a close agreement with data obtained from the experimental study conducted by the authors.[4] In the present work, the turbulent flow analysis of the erosive burning problem is performed for the axisymmetric flow of gases inside a cylindrical propellant grain. The analysis includes the effects of acceleration of the gases due to pressure gradients, and considers both the developing and fully developed regions of the flow. The flowfield inside a nonuniform port diameter of the grain can also be analyzed by means of the present model. These are some of the new features of the model, which are lacking in the previous models,[3,5] based on turbulent flow analysis of the problem.

The objectives of the present study are: 1) to formulate a theoretical model for the erosive burning problem of composite solid propellants by analyzing the flow in a cylindrical rocket motor; and 2) to solve the theoretical model and to perform a parametric study of the effects of gasdynamic operating conditions on erosive burning.

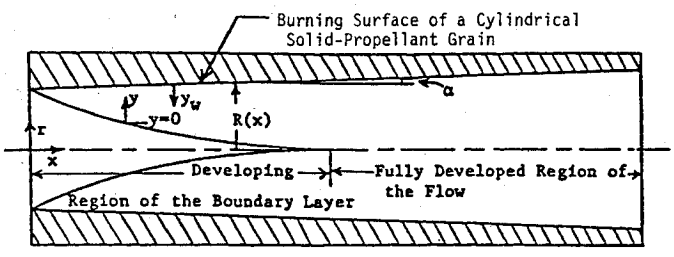

Fig. 1 Physical model considered in the theoretical formulation.

Analysis

Description of Physical Model

The physical model considered in the theoretical analysis consists of an axisymmetric flow of gases inside a cylindrical solid-propellant grain, as shown schematically in Fig. 1. The gases form a turbulent boundary layer over the burning surface of the propellant. The analysis considers both developing and fully developed regions of the flow. Whether or not the developing flow region exists in real rocket motors will depend on factors such as initial conditions, grain geometry, and even igniter gas flow characteristics. However, for generality in the model, the developing region is included in the formulation. The coordinate system used in the analysis is shown in Fig. 1. In this figure, the $x=0$ point does not represent the head end of a grain port but a point from which the boundary layer starts to develop. The analysis is limited to the combustion of commonly used ammonium perchlorate (AP) composite propellants burning in the turbulent boundary-layer region of a rocket motor. It should be noted that the region of turbulent flow usually encompasses the major length of a rocket motor.

Conservation Equations

In the viscous flow region of the boundary layer, Reynolds' decomposition and time-averaging procedure is used to develop the conservation equations. A second-order two-equation K-ϵ turbulence model[6] is used to achieve the closure of the turbulent flow problem. Major assumptions made in the analysis are: 1) averaged flow properties are steady, 2) mean flow is axisymmetric, 3) there is no reaction-generated turbulence, 4) the Lewis number is unity, and 5) Fick's law of diffusion is valid. Boundary-layer equations of mass, momentum, species, enthalpy, turbulence kinetic energy and turbulence dissipation, and the equation of state are, respectively, written below.

$$\frac{\partial}{\partial x}(r\bar{\rho}\bar{u}) + \frac{\partial}{\partial r}(r\bar{\rho}\bar{v}^\circ) = 0 \tag{1}$$

where

$$\bar{\rho}\bar{v}^\circ = \bar{\rho}\bar{v} + \overline{\rho' v'}$$

$$\bar{\rho}\bar{u}\frac{\partial\bar{u}}{\partial x} + \bar{\rho}\bar{v}^\circ\frac{\partial\bar{u}}{\partial r} = \frac{1}{r}\frac{\partial}{\partial r}\left[r\mu_{\text{eff}}\frac{\partial\bar{u}}{\partial r}\right] - \frac{d\bar{p}}{dx} \tag{2}$$

$$\bar{\rho}\bar{u}\frac{\partial\bar{Y}_k}{\partial x} + \bar{\rho}\bar{v}^\circ\frac{\partial\bar{Y}_k}{\partial r} = \frac{1}{r}\frac{\partial}{\partial r}\left[r\left(\frac{\mu}{Sc}\right)_{\text{eff}}\frac{\partial\bar{Y}_k}{\partial r}\right] + \bar{\dot{\omega}}_k \tag{3}$$

$$\bar{\rho}\bar{u}\frac{\partial\bar{H}}{\partial x} + \bar{\rho}\bar{v}^\circ\frac{\partial\bar{H}}{\partial r} = \frac{1}{r}\frac{\partial}{\partial r}\left\{r\left[\left(\frac{\mu}{Pr}\right)_{\text{eff}}\frac{\partial\bar{H}}{\partial r} + \left\{\mu_{\text{eff}} - \left(\frac{\mu}{Pr}\right)_{\text{eff}}\right\}\frac{\partial\bar{u}^2/2}{\partial r}\right]\right\} \tag{4}$$

$$\bar{\rho}\bar{u}\frac{\partial K}{\partial x} + \bar{\rho}\bar{v}^\circ\frac{\partial K}{\partial r} = \frac{1}{r}\frac{\partial}{\partial r}\left[r\left(\mu + \frac{\mu_t}{C_l}\right)\frac{\partial K}{\partial r}\right] + \mu_t\left(\frac{\partial\bar{u}}{\partial r}\right)^2 - \bar{\rho}\epsilon \tag{5}$$

$$\bar{\rho}\bar{u}\frac{\partial\epsilon}{\partial x}+\bar{\rho}\bar{v}^{\circ}\frac{\partial\epsilon}{\partial r}=\frac{1}{r}\frac{\partial}{\partial r}\left[r\left(\mu+\frac{\mu_t}{C_2}\right)\frac{\partial\epsilon}{\partial r}\right]$$

$$+C_3\mu_t\left(\frac{\partial\bar{u}}{\partial r}\right)^2\frac{\epsilon}{K}-C_4\bar{\rho}\frac{\epsilon^2}{K} \tag{6}$$

$$\bar{p}=\bar{\rho}R_u\bar{T}/W \tag{7}$$

Turbulent viscosity μ_t is expressed in terms of K and ϵ as

$$\mu_t=C_\mu\bar{\rho}(K^2/\epsilon) \tag{8}$$

Models for various correlations have been replaced in Eqs. (2-6). These models were discussed by the authors in Ref. 3.

In the potential flow region of the developing flow, the following equations are considered for momentum and energy

$$\rho_c U_c\frac{\mathrm{d}U_c}{\mathrm{d}x}=-\frac{\mathrm{d}\bar{p}}{\mathrm{d}x} \tag{9}$$

$$T_c=T_{tc}\left(1+\frac{\gamma-1}{2}M_c^2\right) \tag{10}$$

Equation (10) is a consequence of isentropic assumption. The centerline velocity U_c is calculated from Eq. (9) and the axial pressure gradient is calculated from the overall momentum balance, using the following equations

$$-\frac{\mathrm{d}\bar{p}}{\mathrm{d}x}=\left[2\pi R\tau_w+\frac{\mathrm{d}}{\mathrm{d}x}(\rho_b A U_b^2)\right]\Big/A \tag{11}$$

$$\frac{\mathrm{d}}{\mathrm{d}x}(\rho_b U_b A)=2\pi R\rho_s r_b \tag{12}$$

Equation (12) is obtained from the overall mass balance inside a rocket motor. The pressure gradient expressed by Eq. (11) includes the effects of change in the flow area and the change in bulk density ρ_b along the x direction.

For chemical reactions in the gas phase, the following single-step forward reaction is assumed

$$\nu_F F+\nu_O O\rightarrow\nu_P P \tag{13}$$

The reaction is assumed to be diffusion-controlled, and the reaction rate expression is based on the eddy breakup model of Spalding.[7,8] Relevance of the eddy breakup model to the turbulent flow analysis of the problem was fully discussed by the authors in Ref. 3. The reaction rate expression can be written as

$$\bar{\dot{\omega}}_F=-C_\omega\bar{\rho}\sqrt{K}\left|\frac{\partial\bar{Y}_F}{\partial r}\right| \tag{14}$$

The main restriction in using Eq. (14) is its applicability to a turbulent flow situation, which is the case in the present problem. With the assumption of Eq. (13), the species conservation equations are solved for $\bar{Y}_F$ and $\bar{Y}_{OF}\equiv[\bar{Y}_O-(\nu_O W_O/\nu_F W_F)\bar{Y}_F]$. The introduction of the latter variable eliminates the nonlinear source term in the equation for $\bar{Y}_{OF}$.

Boundary Conditions

At the solid-gas interface, mass and energy balances lead to the following boundary conditions:

$$(\bar{\rho}\bar{v}\bar{Y}_O)_{r=R}-\rho_s r_b Y_{OS}+\left(\rho\mathcal{D}\frac{\partial\bar{Y}_O}{\partial r}\right)_{r=R}=0 \tag{15}$$

$$(\bar{\rho}\bar{v}\bar{Y}_F)_{r=R}-\rho_s r_b Y_{FS}+\left(\bar{\rho}\mathcal{D}\frac{\partial\bar{Y}_F}{\partial r}\right)_{r=R}=0 \tag{16}$$

$$\lambda\frac{\partial\bar{T}}{\partial r}\Big|_{r=R}=\lambda_s\frac{\partial T_p}{\partial r}\Big|_{r=R}-\rho_s r_b[(C_p-C_s)(T_{ps}-\bar{T}_{ps})+\bar{Q}_s] \tag{17}$$

where $\bar{Q}_s$ in Eq. (17) is defined (following Levine and Culick[9]) as the net surface heat release (negative for exothermic reactions) at a reference temperature $\bar{T}_{ps}$. The net heat flux to the solid propellant is obtained by integrating the heat conduction equation in the solid phase,

$$-\lambda_s\frac{\partial T_p}{\partial r}\Big|_{r=R}=(T_{ps}-T_{pi})\rho_s C_s r_b \tag{18}$$

The burning rate of the solid propellant is expressed as a function of surface temperature through the use of the Arrhenius law of surface pyrolysis

$$r_b=A_s\exp\left(-\frac{E_{as}}{R_u T_{ps}}\right) \tag{19}$$

For K and ϵ equations, Eqs. (5) and (6), the following boundary conditions are applied

$$K=\frac{\ell^2}{\sqrt{C_\mu}}\left(\frac{\partial\bar{u}}{\partial r}\right)^2 \tag{20}$$

$$\epsilon=\ell^2\left|\frac{\partial\bar{u}}{\partial r}\right|^3 \tag{21}$$

These boundary conditions are applied near the propellant surface at $y_+=15$ (see Refs. 3 and 10) rather than directly at the surface to avoid the low-turbulence Reynolds number region in which the application of K and ϵ equations is inappropriate. It should be noted that $y_+=15$ represents a distance of less than 10 μm from propellant surface at the typical rocket motor conditions used in the present calculations. Turbulence viscosity μ_t close to the wall is calculated from van Driest's formula[11] as modified by Cebeci and Chang[12] to include the effect of surface roughness

$$\mu_t=\bar{\rho}\ell^2\left|\frac{\partial\bar{u}}{\partial r}\right| \tag{22}$$

where

$$\ell\equiv k(y_w+\Delta y_w)\left\{1-\exp\left[-\frac{(y_w+\Delta y_w)\bar{\rho}u_*}{A^+\mu}\frac{\tau}{\tau_w}\right]\right\} \tag{23}$$

$$\Delta y_w\equiv 0.9(\mu/\bar{\rho}u_*)[\sqrt{R_h^+}-R_h^+\exp(-R_h^+/6)] \tag{24}$$

$$R_h^+\equiv\rho u_* R_h/\mu \tag{25}$$

In Eq. (23), τ/τ_w is written without the normally used square root in van Driest's formula. This modification has been shown to give better results (see Ref. 13). Other boundary conditions at the propellant surface ($r=R$) are

$$\bar{u}=0,\quad \bar{T}=\bar{T}_{ps},\quad \bar{v}=-\rho_s r_b/\bar{\rho}(x,R) \tag{26}$$

and at the edge of the boundary layer ($y=0$) are

$$\bar{u}=U_c,\quad \bar{T}=T_c,\quad \bar{Y}_F=\bar{Y}_O=0,\quad \frac{\partial K}{\partial r}=\frac{\partial\epsilon}{\partial r}=0 \tag{27}$$

Numerical Method

The coordinate transformation and numerical scheme proposed by Patankar and Spalding[14] was used in this study. Solutions of the differential equations were obtained by numerically integrating the equations along the transverse direction, while marching forward along the x direction (see

Table 1 Properties used in theoretical calculations

$a = 0.245$ cm/s/(MPa)^n	$A_s = 5.65$ m/s
$A^+ = 26$ (Ref. 11)	$C_s = 0.3$ kcal/kg·K
$C_p = 0.3$ kcal/kg·K	$E_{as} = 15$ kcal/mole
$\Delta h^\circ_{f,F} = 55.9$ kcal/kg	$\Delta h^\circ_{f,O} = -942$ kcal/kg
$\Delta h^\circ_{f,p} = -1137.3$ kcal/kg	$k = 0.41$
$n = 0.41$	$Pr = \gamma/(1.77\gamma - 0.45)$ Svehla's equation[16]
$Pr_t = 0.9$	$\bar{Q}_s = -250$ kcal/kg
$Sc = Pr$	$Sc_t = 0.9$
$T_{pi} = 298$ K	$\bar{T}_{ps} = 800$ K
$W_F = 30$ kg/kmole	$W_O = 27.9$ kg/kmole
$W_p = 20.4$ kg/kmole	$Y_{FS} = 0.25$
$Y_{OS} = 0.75$	$\gamma = 1.26$
$\lambda = C_P\mu/Pr$, kcal/m·s·K	$\mu_k = 8.7 \times 10^{-8} \sqrt{W_k} T^{0.65}$ (Ref. 16)
$\nu_F = 1$ kmole	$\nu_O = 3.23$ kmole
$\nu_p = 5.9$ kmole	$\rho_s = 1600$ kg/m^3

Table 2 Contants used in turbulence modeling

Constants	C_1	C_2	C_3	C_4	C_ω	C_μ
Values	1.0	1.3	1.57	2.0	0.18	0.09

Ref. 15 for details). About half of the 100 cross-stream intervals employed were distributed within 10% of the boundary-layer thickness, where the dependent variables change rapidly. Because of strong interaction between the potential core and the viscous boundary layer caused by the axial pressure gradient, a small forward step was taken along the x direction, typically about 0.2 times the boundary-layer thickness. The size of this step was reduced during the forward-marching computation if changes in the U_c and T_c calculations from Eqs. (9) and (10) exceeded specified limits. Iterations of the boundary-layer solutions were performed to obtain convergence on the surface temperature. The maximum allowable error in the convergence of the surface temperature was set at 0.01%.

Results

Physical Properties Used in Calculations

Theoretical solutions were obtained for a composite propellant composed of 75% ammonium perchlorate and 25% PBAA/EPON by weight. Various physical properties used in the calculations and the references from which some of the properties were taken are listed in Table 1. The procedure followed in obtaining some of the parameters associated with the global single-step forward reaction has been discussed in detail in Ref. 3. Values of the constants used in the turbulence modeling are given in Table 2 and sources of the constants are given in Ref. 3.

Computations were started at a preselected downstream x location in the turbulent region of the boundary layer. The downstream x location in most calculations was chosen to be 0.24 m, and the initial boundary-layer thickness was computed from a correlation in terms of the Reynolds number based on this value of x. The starting profiles for velocity and turbulent kinetic energy and dissipation were obtained by using the same equations used by Chambers and Wilcox.[10] The initial centerline velocity was varied for the parametric study.

Results and Discussion

Figure 2 shows the calculated distributions of velocity (nondimensionalized with initial centerline velocity) at various distance-to-diameter ratios, x/D. Velocity gradient increases with the downstream distance, since the flow inside the rocket motor is accelerated by the strong favorable pressure

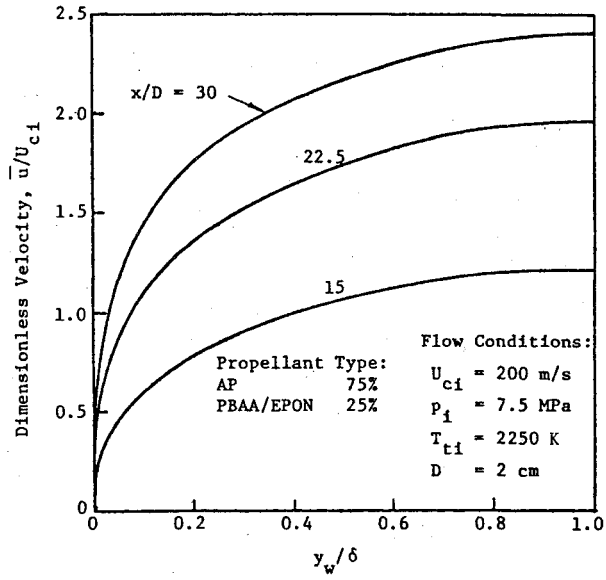

Fig. 2 Calculated velocity distributions in the boundary layer at various axial locations.

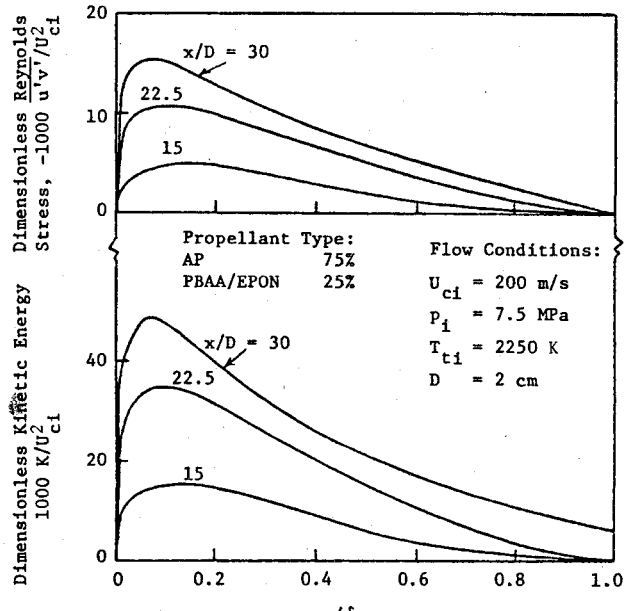

Fig. 3 Calculated distributions of turbulent kinetic energy and Reynolds stress in the boundary layer at various axial locations.

gradient. In Fig. 2, $x/D = 30$ station is in the fully developed region. The kinetic energy and Reynolds stress profiles at the corresponding x/D stations are shown in Fig. 3. Since the velocity gradient increases with distance x, a corresponding increase occurs in both K and $\overline{u'v'}$ with increasing x. Figure 3 also shows that the distance between the peak turbulent kinetic energy and the propellant surface decreases as the flow accelerates in the downstream direction. This was also observed in the simulative study of erosive burning made by Yamada et al.[17] Thus, with increasing distance x, more turbulence activity occurs closer to the propellant surface, enhancing the mixing processes and the reaction rate [Eq. (14)] near the surface.

The increased reaction rate effect is evident from the results plotted in Fig. 4, which shows the calculated distribution of average fuel and oxidizer mass fractions and the rate of heat generation in the gas phase near the propellant surface. With the increase in x/D, the peak value of the heat generation rate increases in magnitude and its location becomes closer to the propellant surface. This indicates a strong interaction between

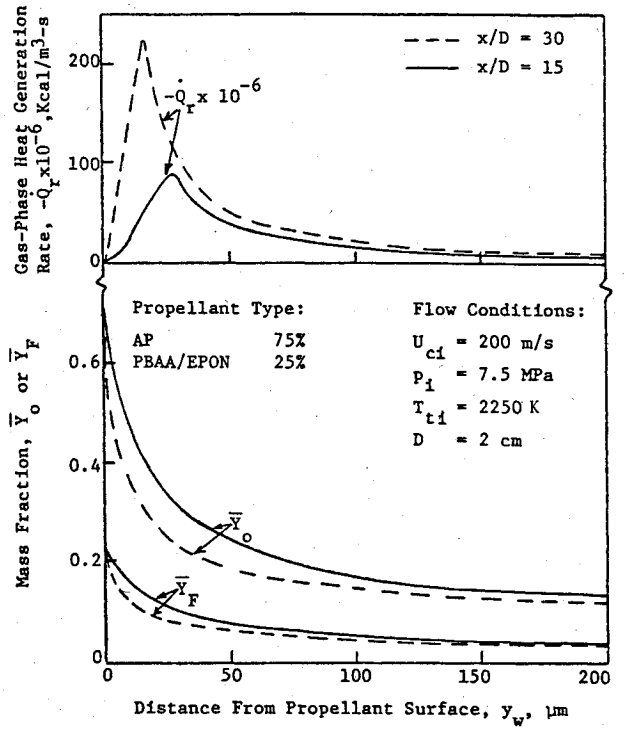

Fig. 4 Calculated distribution of oxidizer and fuel mass fractions, and the rate of heat generation in the gas phase near the propellant surface.

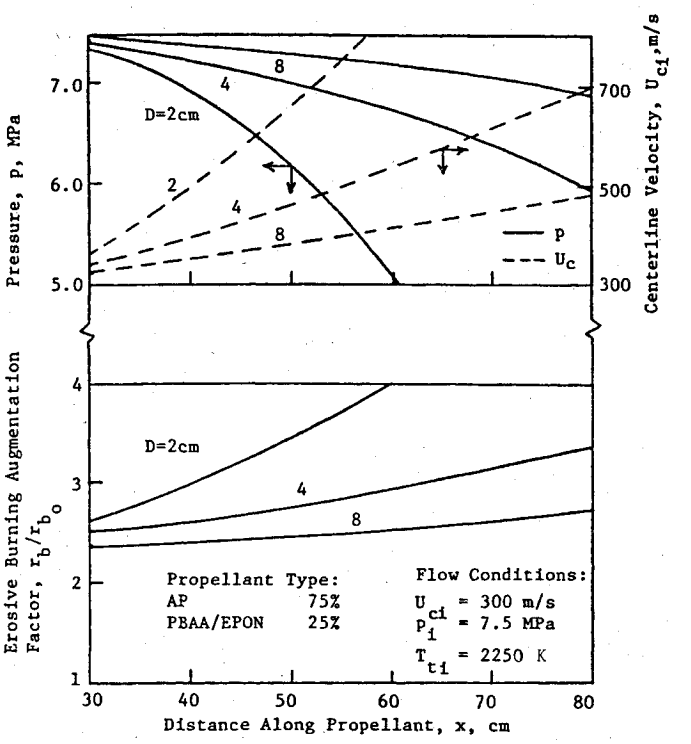

Fig. 6 Calculated variations in pressure, centerline velocity, and erosive burning augmentation factor along axial direction for different port diameters of rocket motors.

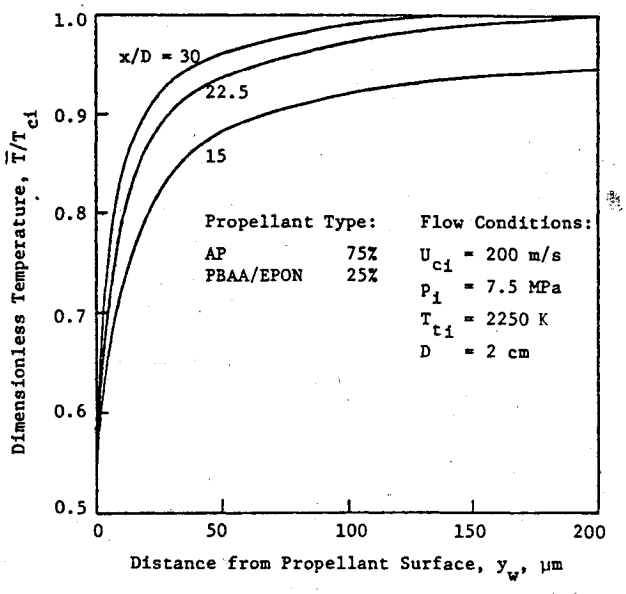

Fig. 5 Calculated temperature distributions near the propellant surface at different axial locations.

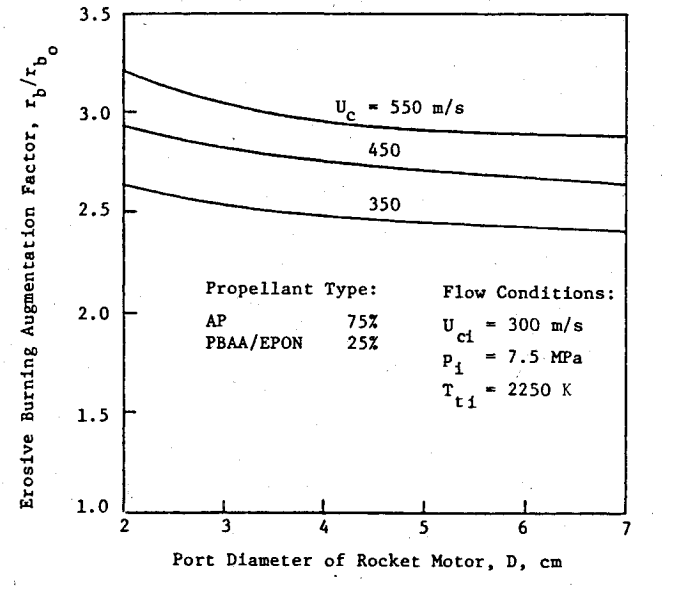

Fig. 7 Effect of port diameter on erosive burning augmentation factor at different centerline velocities.

turbulence and the gas-phase reaction rate. Due to the higher reaction rate at $x/D = 30$, as compared to that at $x/D = 15$ in Fig. 4, the mass fractions of both fuel and oxidizer species decrease faster in the direction away from the propellant surface. The temperature gradient steepens as a consequence of the increase in the reaction rate; this can be seen from the calculated temperature distributions plotted near the propellant surface in Fig. 5 at various x/D values. The higher temperature gradient with increasing x/D means higher gas-to-solid heat flux and, therefore, increased burning rate as x/D increases.

The erosive burning augmentation factor, r_b/r_{b_0}, is plotted as a function of x for different port diameters of a rocket motor in Fig. 6. It is seen that r_b/r_{b_0} increases as x increases.

Figure 6 also shows the variation of pressure and centerline velocity with distance x. With a favorable pressure gradient, the pressure decreases while the centerline velocity increases. The results given in Fig. 6 also indicate that decreasing the port diameter causes r_b/r_{b_0} to increase. However, this increase is caused by the changes in both port diameter and x location (centerline velocity). In order to emphasize the port diameter effect, results of r_b/r_{b_0} are plotted in Fig. 7 as a function of port diameter for a number of fixed centerline velocities. In this way, the effect of x variation of U_c on r_b/r_{b_0} is eliminated and the port diameter effect is isolated. The results again show that a decrease in port diameter makes a rocket motor more sensitive to erosive burning. This conclusion is in agreement with the study conducted by Beddini.[5]

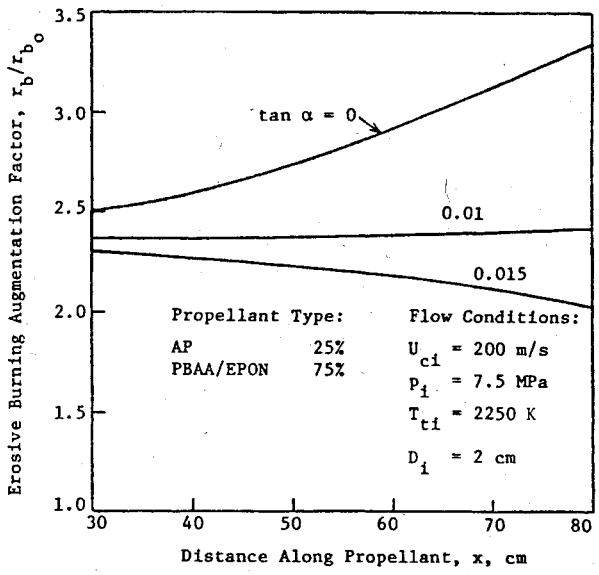

Fig. 8 Effect of nonuniform port diameter on erosive burning augmentation factor.

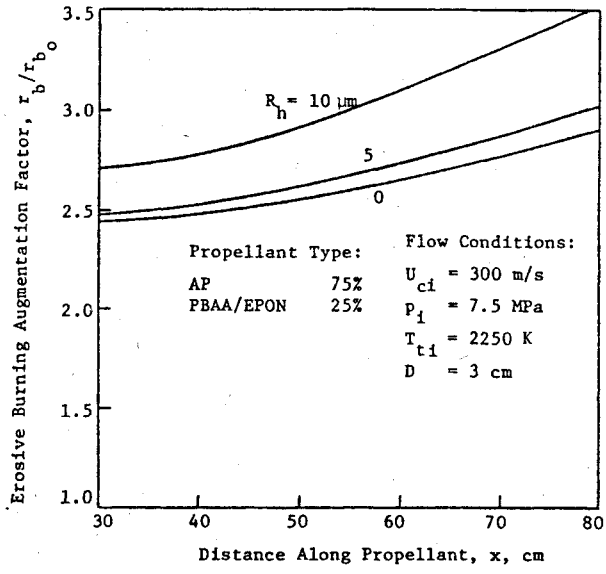

Fig. 9 Calculated erosive burning augmentation factor showing the effect of propellant surface roughness.

Figure 8 shows a very interesting result of the effect of nonuniform diameter along x on the erosive burning augmentation factor. The results have been plotted for $\tan\alpha = 0$, 0.01, and 0.015, where α is the divergence angle of the rocket motor grain (see Fig. 1). As is well known, the erosive burning effect is usually strong in the initial burning phase of a rocket motor when the diameter is nearly uniform. This corresponds to $\tan\alpha = 0$ in Fig. 8 (D being constant along x); r_b/r_{b_0} increases significantly as the flow accelerates in the x direction. However, when $\tan\alpha > 0$, r_b/r_{b_0} behavior changes significantly along x, as depicted in Fig. 8. With $\tan\alpha = 0.01$, there is less acceleration and, therefore, the erosive burning effect remains more or less constant as x increases. With $\tan\alpha = 0.015$, r_b/r_{b_0} is seen to decrease as x increases; this is due to the effects of the thickening boundary layer. In sharp contrast to the effect of acceleration, the effect of the thickening boundary layer is to reduce r_b/r_{b_0}. Therefore, depending upon the grain geometry, the erosive burning effect could either increase or decrease in the axial direction toward the aft end of a rocket motor.

Figure 9 shows the effect of propellant surface roughness on the erosive burning augmentation factor. Increasing the height of the roughness increases the augmentation factor. This is consistent with the experimental study conducted by the authors,[4] which showed a larger erosive burning effect on a composite propellant with larger surface roughness due to larger AP particle size.

Summary and Conclusions

1) The problem of erosive burning of composite solid propellants was modeled by considering an axisymmetric turbulent boundary layer inside a rocket motor. The theoretical model was solved numerically, and a parametric study for the effect of a number of important variables was conducted.

2) The erosive burning augmentation factor increases with the increase in axial distance when the port diameter of the rocket motor is uniform (representing an initial time period immediately following the ignition in a rocket motor). For a nonuniform (diverging) port diameter, the augmentation factor increases at a lesser rate, and even decreases with increasing x if divergence is large.

3) Rocket motors with a smaller port diameter are more sensitive to erosive burning than those with larger diameters.

4) Surface roughness increases the erosive burning effect of a composite solid propellant.

5) Mechanism of erosive burning is believed to be caused by increased turbulence activity near the propellant surface as the axial velocity is increased. The increased turbulence activity increases both the mixing process and the reaction rate within the gas phase near the propellant surface.

Acknowledgments

This work represents a part of the research performed under a subcontract from the Atlantic Research Corporation which was the prime contractor for the Air Force Office of Scientific Research, Contract F49620-78-C-0016, under the management of Capt. R. F. Sperlein and Dr. L. H. Caveny.

References

[1] Kuo, K. K. and Razdan, M. K., "Review of Erosive Burning of Solid Propellants," *12th JANNAF Combustion Meeting*, CPIA Pub. 273, Vol. II, 1975, pp. 323-338.

[2] King, M. K., "Review of Erosive Burning Models," Paper presented at JANNAF Workshop on Erosive Burning/Velocity Coupling, Lancaster, Calif., March 1977.

[3] Razdan, M. K. and Kuo, K. K., "Erosive Burning Study of Composite Solid Propellants by Turbulent Boundary-Layer Approach," *AIAA Journal*, Vol. 17, Nov. 1979, pp. 1225-1233.

[4] Razdan, M. K. and Kuo, K. K., "Measurements and Model Validation for Composite Propellants Burning under Cross Flow of Gases," *AIAA Journal*, Vol. 18, June 1980, pp. 669-677.

[5] Beddini, R. A., "Reacting Turbulent Boundary-Layer Approach to Solid Propellant Erosive Burning," *AIAA Journal*, Vol. 16, Sept. 1978, pp. 898-905.

[6] Launder, B. E. and Spalding, D. B., *Mathematical Models of Turbulence*, Academic Press, New York, 1972, p. 9.

[7] Spalding, D. B., "Mixing and Chemical Reaction in Steady Confined Turbulent Flames," *Thirteenth Symposium (International) on Combustion*, The Combustion Institute, Pittsburgh, Pa., 1971, pp. 649-657.

[8] Mason, H. B. and Spalding, D. B., "Prediction of Reaction Rates in Turbulent Pre-Mixed Boundary Layer Flows," *First European Symposium*, The Combustion Institute, Pittsburgh, Pa., 1973, pp. 601-606.

[9] Levine, J. N. and Culick, F.E.C., "Nonlinear Analysis of Solid Rocket Combustion Instability," AFRPL-TR-74-45, Final Rept., Vol. I, 1974.

[10] Chambers, T. L. and Wilcox, D. C., "Critical Examination of Two-Equation Turbulence Closure Models for Boundary Layers," *AIAA Journal*, Vol. 15, June 1977, pp. 821-828.

[11] van Driest, E. R., "On Turbulent Flow Near a Wall," *Journal of the Aeronautical Sciences*, Vol. 23, 1956, pp. 1007-1011.

[12] Cebeci, T. and Chang, K. C., "Calculation of Incompressible Rough-Wall Boundary-Layer Flows," *AIAA Journal*, Vol. 16, July 1978, pp. 730-735.

[13] Baker, R. J. and Launder, B. E., "The Turbulent Boundary Layer with Foreign Gas Injection, II: Predictions and Measurements in Severe Streamwise Pressure Gradients," *International Journal of Heat and Mass Transfer*, Vol. 17, 1974, pp. 293-306.

[14] Patankar, S. V. and Spalding, D. B., *Heat and Mass Transfer in Boundary Layers*, Inter-text Books, London, 1970.

[15] Razdan, M. K. and Kuo, K. K., "Turbulent Boundary-Layer Analysis and Experimental Investigation of Erosive Burning Problem of Composite Solid Propellants," AFOSR-TR-79-1155, Scientific Rept. to U.S. Air Force Office of Scientific Research, March 1979.

[16] Peretz, A., Kuo, K. K., Caveny, L. H., and Summerfield, M., "Starting Transient of Solid Propellant Rocket Motors with High Internal Gas Velocities," *AIAA Journal*, Vol. 11, Dec. 1973, pp. 1719-1727.

[17] Yamada, K., Goto, M., and Ishikawa, N., "Simulative Study on the Erosive Burning of Solid Rocket Motors," *AIAA Journal*, Vol. 14, Sept. 1976, pp. 1170-1177.